Available online at www.sciencedirect.com
SCIENCE DIRECT®
Bioorganic & Medicinal Chemistry 13 (2005) 4842–4850
Bioorganic & Medicinal Chemistry

Synthesis of novel 5-aryl-2-thio-1,3,4-oxadiazoles and the study of their structure–anti-mycobacterial activities

Fliur Macaev,[a,*] Ghenadie Rusu,[a] Serghei Pogrebnoi,[a] Alexandru Gudima,[a] Eugenia Stingaci,[a] Ludmila Vlad,[a] Nathaly Shvets,[b] Fatma Kandemirli,[c] Anatholy Dimoglo[a,b,*] and Robert Reynolds[d]

[a]*Institute of Chemistry, Academy of Sciences of Moldova, Chisinau, MD-2028, Republic of Moldova*
[b]*Gebze Institute of Technology, 41400, Turkey*
[c]*Kocaeli University, 41400, Turkey*
[d]*Southern Research Institute, Birmingham, AL 35255-5305, USA*

Received 13 April 2005; revised 5 May 2005; accepted 6 May 2005

Abstract—The preparation of novel 5-aryl-2-thio-1,3,4-oxadiazoles **4a**–**41** and the computer-aided study of their in vitro anti-tubercular activity against *Mycobacterium tuberculosis* $H_{37}Rv$ (ATCC 27294) are reported. The average accuracy of the electronic-topological method and neural network methods applied to the activity prediction in leave-one-out cross validation is 80%.

1. Introduction

Data from the World Organization of Health show a significant rise in drug-resistant tuberculosis.[1–3] Tuberculosis (TB) is one of the leading causes of death and suffering worldwide among the infectious diseases. The ever-increasing drug resistance, toxicity and side effects of currently used anti-tuberculosis drugs and the absence of their bactericidal activity highlight the need for new, safer and more effective anti-tuberculosis drugs.[4–8] The computer-aided prediction of biological activity in relation to the chemical structure of a compound is now a commonly used technique in drug discovery.[9–14] Modern drug discovery also relies on the interface of chemical and biological diversity through high throughput screening.[15] Generation of functional molecular diversity to probe biological activity space requires robust molecular scaffolds that are low in molecular weight and are easily modified to create a variety of chemically diverse, biologically active potential drugs.[16,17] We also report our efforts to relate the dependence of the anti-mycobacterial activity of new compounds on the nature of substitution in the 5-aryl-2-thio-1,3,4-oxadiazoles **4a**–**41**.

The present study uses both the electronic-topological method (ETM) and neural network (NN) methods to predict anti-tuberculosis activity. The better the description of a molecule in terms of structural parameters representing its activity, the better the results of pattern recognition and separation of the molecules by activity. The ETM is a structure-based approach for studying structure–activity relationships (SAR) of molecules.[18] ETM is also capable of taking into account individual properties of separate atoms and bonds that may be crucial for revealing details of interactions between a biologic receptor and an active molecule. A number of studies have been reported that use the ETM to find SAR models involving a representative list of activities and thousands of compounds belonging to different chemical classes.[19–22] The ETM approach and software have both undergone considerable development.[23] The new ETM-based system capable of unifying Web-based SAR resources and using Internet communications in the framework of a project, ETOSAR, makes the ETM a valuable tool for SAR studies and provides rules for the synthesis of new potentially active compounds.

Keywords: Anti-tubercular activity; 5-Aryl-2-thio-1,3,4-oxadiazoles; Structure–activity relationships; Electronic-topological method; Neural network method.
* Corresponding authors. Tel.: +90 262 653 84 97/1428; fax: +90 262 653 84 90; e-mail addresses: flmacaev@cc.acad.md; dimoglo@gyte.edu.tr

0968-0896/$ - see front matter © 2005 Elsevier Ltd. All rights reserved.
doi:10.1016/j.bmc.2005.05.011

For the analysis of data on the pharmacophores in this study we have used one of the most well known NN—the feed forward neural networks (FFNNs) trained with the back propagation algorithm.[24,25]

2. Chemistry and biological activity testing

This chemistry utilizes different benzoic acids **1a–j** as starting materials. The synthesis of targets 1,3,4-oxadiazoles **4a–41** was accomplished, following a four-step synthetic route according to Scheme 1. The synthesized compounds are given in Table 1.

Hydrazinolysis of esters **2a–j** with 100% hydrazine hydrate in refluxing EtOH gave the corresponding hydrazides **3a–j**. We have reported earlier that arylhydrazines react with tetramethylthiuram disulfide (TMTD) in DMF to form 5-aryl-2-thio-1,3,4-oxadiazoles.[26] During the course of this study, compounds **3a–j** were cyclized into thiols **4a–j** with TMTD in DMF by the reported procedure.

The synthesis of 2-*R*-thio-5-phenyl-1,3,4-oxadiazoles **5–23** and **25–39** was carried out in acetone or DMF, depending on the nature of the alkylating reagent. For example, reaction of thiol **4a–j** with various ω-bromoacetophenones was carried out at room temperature in acetone in the presence of Et_3N. The synthesis of new 1,3,4-oxadiazoles **25–39** as the carbonyl-protected analogs of compound **7–23** by alkylation of oxadiazole **4a–j** with the corresponding 2-phenyl-2-bromomethyl-1,3-dioxolanes in DMF/K_2CO_3 at elevated temperature is depicted in Scheme 1. Allylic bromination of compound **7** by NBS following condensation of product **24** with thiourea gave the 2-aminothiazole **41**. Under Knoevenagel conditions, a condensation of **7** with *p*-Br-benzaldehyde was preformed, and compound **40** was obtained as the main reaction product. All compounds were obtained with high yields. Physical, analytical and spectral data are presented in Tables 2 and 3.

The synthesized compounds **4a–41** in the present study were tested for the in vitro anti-mycobacterial activity against *Mycobacterium tuberculosis* $H_{37}Rv$ using the Alamar Blue assay method.[15] Predicted and experimentally-measured percent inhibition (PI—relative inhibition of bacterial growth at 6.25 μg/mL) values for the synthesized compounds against *M. tuberculosis* $H_{37}Rv$ are given in Table 1. Rifampicin was used as the control standard in the assays for in vitro inhibition of *M. tuberculosis* $H_{37}Rv$.

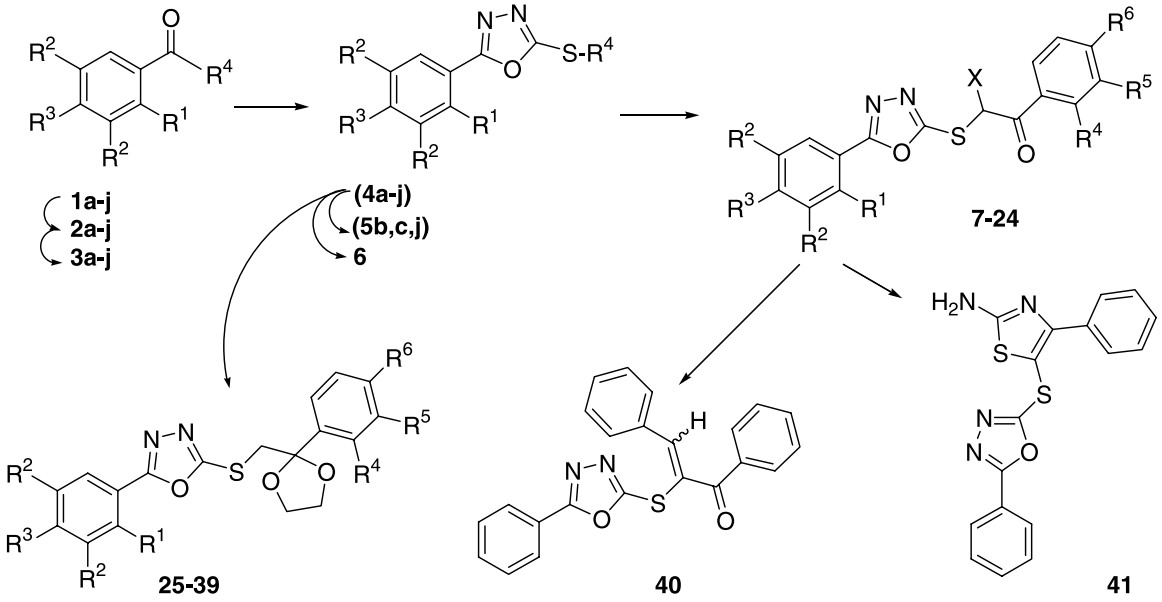

R^1=H (1a, 1g-j, 2a, 2g-j, 3a, 3g-j, 4a, 4g-j, 5j, 6); **OH** (1b, 2b, 3b, 4b, 5b); **Br** (1c, 2c, 3c, 4c, 5c);
Me (1d, 2d, 3d, 4d); **Cl** (1e, 2e, 3e, 4e);
R^1=R^3=Cl, R^2=H (1f, 2f, 3f, 4f);
R^2=H (1g, 1h, 1i, 2g, 2h, 2i, 3g, 3h, 3i, 4g, 4h, 4i);
R^3=OH (1g, 2g, 3g, 4g); **OMe** (1h, 2h, 3h, 4h); **OEt** (1i, 2i, 3i, 4i);
R^2=R^3=OMe (1j, 2j, 3j, 4j, 5j);
R^4=OH (1a-j); **OMe** (2a-j); **$NHNH_2$** (3a-j); **H** (4a-j); **Me** (5b, 5c, 5j).

Scheme 1. The synthesis of compounds **2a–41**.

Table 1. Synthesized compounds and anti-mycobacterial activity against *M. tuberculosis* $H_{37}Rv$ (in vitro)

Compound	R^1	R^2	R^3	R^4	R^5	R^6	Inhibition (%)	Prediction (%)
4f	CI	H	CI	H	—	—	20	19
4j	H	OMe	OMe	H	—	—	3	4
5b	OH	H	H	Me	—	—	30	35
5c	Br	H	H	Me	—	—	47	37
5f	H	OMe	OMe	Me	—	—	20	19
6	H	OMe	OMe	CH_2Py	—	—	39	35
7	H	H	H	H	H	H	28	23
8	OH	H	H	H	H	H	45	54
9	Me	H	H	H	H	H	19	19
10	CI	H	H	H	H	H	17	13
11	H	H	H	H	H	F	58	54
12	H	OMe	OMe	H	H	F	27	30
13	H	H	H	H	H	NO_2	24	31
14	H	OMe	OMe	H	H	Br	22	32
15	H	OMe	OMe	Cl	H	CI	12	7
16	H	OMe	OMe	H	OMe	H	17	20
17	H	OMe	OMe	H	H	Me	48	36
18	H	OMe	OMe	H	H	Phenyl	37	34
19	H	OMe	OMe	H	H	NO_2	33	33
20	H	OMe	OMe	H	H	CI	27	30
21	H	OMe	OMe	H	OMe	OMe	31	30
22	H	OMe	OMe	2-Naphthyl	39	31		
23	H	OMe	OMe	H	H	H	19	31
24[a]	H	H	H	H	H	H	33	43
25	OH	H	H	H	H	F	33	39
26	OH	H	H	2-Naphthyl	15	15		
27	OH	H	H	H	H	Br	13	16
28	H	H	H	H	H	H	82	53
29	OH	H	H	H	H	H	55	37
30	H	H	OEt	H	H	H	0	4
31	H	H	OMe	H	OMe	H	0	4
32	H	H	OMe	H	H	CI	15	14
33	H	H	OH	H	OMe	H	0	3
34	H	H	OH	H	OMe	OMe	3	11
35	H	OMe	OMe	H	H	F	6	4
36	H	OMe	OMe	H	H	Br	7	4
37	H	OMe	OMe	H	H	CI	28	37
38	H	OMe	OMe	H	OMe	H	5	5
39	H	OMe	OMe	H	H	H	14	11
40	H	H	H	H	H	H	30	18
41	H	H	H	H	H	H	55	58

[a] *Note.* X = Br.

In the first part of this study, we investigated dependence of target activity on the nature of substituents in the 1,3,4-oxadiazoles **4f**,**j**; **5b**,**c**,**j** and **6**. Thiol **4j** had the lowest activity (PI 3%). Its methyl ether **5j** and the 2,4-dichloro analog **4f** of **4j** showed 20% higher activity. Salicylic acid derivative **5b** possessed even greater activity (percent inhibition of bacterial growth of 30%). It was found that substituting a halogen (compound **5c**) to hydroxyl group (compound **5b**) increased bioactivity to 17%. The ether **6** of 4-sulfanylmethylpyridine showed activity with a PI of 39%.

In the case of the gallic acid derivatives, the presence of a halogen (**12**, **14**, **20**) leads to a decrease in activity. The maximum activity among 3,4,5-trimethoxy analogs was observed for compound **17**. It was noted that decreasing the number of methoxy groups to one in the aromatic ring of 5-aryl-1,3,4-oxadiazole **38** reduces its activity to only 5% inhibition. The fluoro-substituted product **11** showed the highest activity among the derivatives of benzoic acid **7–11**, **13**. Salicylic acid derivative **29** with a similar structure showed practically the same level of activity and was the most active among the ortho-hydroxy compounds. Chloride **10** was less active than the analogous non-halogenated product **7**. It was found that 1,3-dioxolane derivatives are less active than the corresponding keto-precursor compounds. Compounds **29** and **28** are notable exceptions. The latter showed the highest target activity (82%) among all the 5-aryl-2-thio-1,3,4-oxadiazoles derived from benzoic acids **1a**–**j**.

3. Results and discussion

3.1. The search for pharmacophores (Ph) and anti-pharmacophores (APh) by using ETM

The compounds under study (41 molecules) are shown in Table 1. Molecules were classified as *active* (21 compounds showing PI $\geqslant$ 24), and *inactive* (20 compounds

Table 2. Physical and analytical data of synthesized compounds **3a**–**41**

Compound	Mp (°C) from EtOH[a]	Yield (%)	Molecular formula	Elemental analyses (%)		
				C, Calcd/Found	H, Calcd/Found	N, Calcd/Found
3a	113–117	94	$C_7H_8N_2O$	61.75/61.52	5.92/6.04	20.58/20.72
3b	147–150	82	$C_7H_8N_2O_2$	55.26/55.19	5.30/5.39	18.41/18.55
3c	150–152	92	$C_7H_7BrN_2O$	39.10/39.02	3.28/3.34	13.03/13.14
3d	Decomp.	92	$C_8H_{10}N_2O$	63.98/63.91	6.71/6.65	18.65/18.72
3e[a]	117–118	87	$C_7H_7ClN_2O$	49.28/49.22	4.14/4.08	16.42/16.48
3f	Decomp.	88	$C_7H_6Cl_2N_2O$	41.00/40.96	2.95/2.91	13.66/13.72
3g	264–266	91	$C_7H_8N_2O_2$	55.26/55.22	5.30/5.26	18.41/18.33
3h	136–140	95	$C_8H_{10}N_2O_2$	57.82/57.77	6.07/5.99	16.86/16.92
3i	129–130	94	$C_9H_{12}N_2O_2$	59.99/59.92	6.71/6.67	15.55/15.48
3j	Decomp.	80	$C_{10}H_{14}N_2O_4$	53.09/53.02	6.24/6.19	12.38/12.31
4a	219–222	90	$C_8H_6N_2OS$	53.92/53.88	3.39/3.42	15.72/15.84
4b	121–214	68	$C_8H_6N_2O_2S$	49.47/49.52	3.11/3.18	14.42/14.52
4c	210–211	87	$C_8H_5BrN_2OS$	37.37/37.48	1.96/2.01	10.90/10.94
4d	Decomp.	91	$C_9H_8N_2OS$	56.23/56.27	4.19/4.24	14.57/14.53
4e	Decomp.	86	$C_8H_5ClN_2OS$	45.18/45.22	2.37/2.44	13.17/13.24
4f	177–178	84	$C_8H_4Cl_2N_2OS$	38.89/38.94	1.63/1.67	11.34/11.38
4g	234–236	72	$C_8H_6N_2O_2S$	49.47/49.52	3.11/3.18	14.42/14.47
4h	Decomp.	81	$C_9H_8N_2O_2S$	51.91/51.96	3.87/3.92	13.45/13.48
4i	175–176	79	$C_{10}H_{10}N_2O_2S$	54.04/54.12	4.53/4.57	12.60/12.64
4j	Decomp.	85	$C_{11}H_{12}N_2O_4S$	49.24/49.29	4.51/4.55	10.44/10.48
5b	73–75	87	$C_9H_8N_2O_2S$	51.91/51.96	3.87/3.82	13.45/13.49
5c	60–62	91	$C_9H_7BrN_2OS$	39.87/39.67	2.60/2.49	10.33/10.42
5j	142–143	92	$C_{12}H_{14}N_2O_4S$	51.05/51.09	5.00/5.03	9.92/9.96
6	Decomp.	76	$C_{17}H_{17}N_3O4S$	56.81/56.70	4.77/4.79	11.69/11.45
7	167–169	93	$C_{16}H_{12}N_2O_2S$	64.85/64.88	4.08/4.12	9.45/9.49
8	195–198	78	$C_{16}H_{12}N_2O_3S$	61.53/6158	3.87/3.92	8.97/8.94
9	139–142	89	$C_{17}H_{14}N_2O_2S$	65.79/65.83	4.55/4.61	9.03/9.10
10	127–129	91	$C_{16}H_{11}ClN_2O_2S$	58.09/58.12	3.35/3.39	8.47/8.52
11	160–162	92	$C_{16}H_{11}FN_2O_2S$	61.14/61.17	3.53/3.58	8.91/8.94
12	159–160	89	$C_{19}H_{17}FN_2O_5S$	56.43/56.48	4.24/4.26	6.93/6.98
13	210–211	79	$C_{16}H_{11}N_3O_4S$	56.30/56.33	3.25/3.28	12.31/12.35
14	199	92	$C_{19}H_{17}BrN_2O_5S$	49.04/49.10	3.68/3.72	6.02/6.09
15	153–155	80	$C_{19}H_{16}Cl_2N_2O_5S$	50.12/50.16	3.54/3.59	6.15/6.19
16	123–125	89	$C_{20}H_{20}N_2O_6S$	57.88/57.92	4.84/4.87	6.73/6.78
17	130–132	79	$C_{20}H_{20}N_2O_5S$	59.99/60.03	5.03/5.08	7.00/7.06
18	166–167	79	$C_{25}H_{22}N_2O_5S$	64.92/64.95	4.79/4.84	6.06/6.11
19	236–237	87	$C_{19}H_{17}N_3O_7S$	52.90/52.94	3.97/4.02	9.74/9.77
20	191–192	88	$C_{19}H_{17}ClN_2O_5S$	54.22/54.26	4.07/4.12	6.66/6.69
21	157–158	84	$C_{21}H_{22}N_2O_7S$	56.49/56.53	4.97/5.03	6.27/6.33
22	156–157	92	$C_{23}H_{20}N_2O_5S$	63.29/63.33	4.62/4.67	6.42/6.48
23	99–101	88	$C_{19}H_{18}N_2O_5S$	59.06/59.02	4.70/4.74	7.25/7.32
24	127–129	90	$C_{16}H_{11}BrN_2O_2S$	51.21/51.17	2.95/2.89	7.47/7.41
25	133–135	71	$C_{18}H_{15}FN_2O_4S$	57.75/57.71	4.04/3.97	7.48/7.54
26	Decomp.	68	$C_{22}H_{18}N_2O_4S$	65.01/64.94	4.46/4.38	6.89/6.94
27	134–136	73	$C_{18}H_{15}BrN_2O_4S$	49.67/49.62	3.47/3.42	6.44/6.53
28[a]	129–130	81	$C_{18}H_{16}N_2O_3S$	63.51/63.55	4.74/4.78	8.23/8.28
29	147–149	65	$C_{18}H_{16}N_2O_4S$	60.66/60.72	4.53/4.57	7.86/7.92
30	Decomp.	88	$C_{20}H_{20}N_2O_4S$	62.48/62.36	5.24/5.11	7.29/7.41
31	98–99	69	$C_{20}H_{20}N_2O_5S$	59.99/60.03	5.03/5.10	7.00/7.05
32	112–114	71	$C_{19}H_{17}ClN_2O_4S$	56.36/56.38	4.23/4.25	6.92/6.95
33	153–154	67	$C_{19}H_{18}N_2O_5S$	59.06/59.11	4.70/4.73	7.25/7.29
34	201–202	68	$C_{20}H_{20}N_2O_6S$	57.68/57.62	4.84/4.78	6.73/6.78
35	128–130	82	$C_{21}H_{21}FN_2O_6S$	56.24/56.28	4.72/4.77	6.25/6.28
36	92–94	81	$C_{21}H_{21}BrN_2O_6S$	49.52/49.56	4.16/4.21	5.50/5.52
37	102–103	76	$C_{21}H_{21}ClN_2O_6S$	54.25/54.28	4.55/4.59	6.03/6.08
38	119–121	77	$C_{22}H_{24}N_2O_7S$	57.38/57.42	5.25/5.29	6.08/6.12
39	148–149	81	$C_{21}H_{22}N_2O_6S$	58.59/58.62	5.15/5.20	6.51/6.55
40	177–178	76	$C_{23}H_{15}BrN_2O_2S$	59.62/59.58	3.26/3.24	6.05/6.12
41	227–229	88	$C_{17}H_{12}N_4OS_2$	57.93/57.88	3.43/3.37	15.90/15.96

[a] *Note.* **3e** from Et_2O; **28** from benzene.

with PI $\leqslant$ 22). Conformational analysis and quantum chemistry calculations were carried out by means of the molecular mechanics method (MMP2) and the semi-empirical quantum chemistry method (AM1), respectively.[27] Diagonal elements of the matrices called electronic-topological matrices of contiguity (ETMC)

Table 3. ^{1}H NMR spectral data of compounds **4a**–**39**

Comp.	δ (ppm)
4a	7.30–8.18 m (5H, arom), 12.4 s (1H, SH)
4b	7.23–7.91 m (4H, arom), 9.68 s, 10.4 s (2H, SH, OH)
4c	7.03–7.85 m (4H, arom), 10.9 s (1H, SH)
4d	2.54 s (3H, Me), 7.49–7.84 m (4H, arom), 9.6 s (1H, SH)
4e	7.26–7.96 m (4H, arom), 11.3 s (1H, SH)
4f	7.38–7.98 m (3H, arom), 10.9 s (1H, SH)
4g	5.12 w s (1H, OH), 7.08 d, 7.18 d (4H, J = 8.46 Hz, arom), 11.4 s (1H, SH)
4h	3.75 s (3H, Me), 7.01 d, 7.97 d (4H, J = 8.46 Hz, arom), 10.1 s (1H, SH)
4i	1.35 t (3H, Me, J = 6.99 Hz), 4.11 q (2H, CH_2, J = 6.88 Hz), 7.53 d, 7.79 d (4H, J = 8.86 Hz, arom), 14.5 s (1H, SH)
4j	3.88 s (9H, 3 Me), 7.72–7.75 m (2H, arom), 13.1 s (1H, SH)
5b	2.59 s (3H, Me), 6.89–7.82 m (4H, arom), 10.28 s (1H, OH)
5e	2.53 s (3H, Me), 7.26–7.93 m (4H, arom)
5j	2.68 s (3H, MeS), 3.76 s (3H, MeO), 3.90 s (6H, 2MeO), 7.18 s (2H, arom)
6	3.77 s (3H, Me), 3.81 s (6H, 2Me), 4.59 s (2H, CH_2), 7.12–7.13 m (4H, arom), 7.48–8.61 m (4H, Py)
7	5.08 s (2H, CH_2), 7.50–8.10 m (10H, arom)
8	5.13 s (2H, CH_2), 6.92–8.12 m (9H, arom), 9.94 s (1H, OH)
9	2.50 s (3H, Me), 5.11 s (2H, CH_2), 7.38–8.20 m (9H, arom)
10	5.18 s (2H, CH_2), 7.43–8.12 m (9H, arom)
11	5.15 s (2H, CH_2), 6.84–8.25 m (9H, arom)
12	3.81 s (3H, Me), 3.83 s (6H, 2Me), 5.10 s (2H, CH_2), 7.16–8.15 m (6H, arom)
13	4.18 s (2H, CH_2), 7.40–8.31 m (9H, arom)
14	3.78 s (3H, Me), 3.81 s (6H, 2Me), 5.19 s (2H, CH_2), 7.19 s (2H, arom), 7.81 d, 8.01 d (4H, J = 8.84 Hz, arom)
15	3.77 s (3H, Me), 3.85 s (6H, 2Me), 4.78 s (2H, CH_2), 7.31–7.92 m (6H, arom)
16	3.76 s (3H, Me), 3.81 s (9H, 3Me), 5.14 s (2H, CH_2), 6.87–8.12 m (6H, arom)
17	2.46 s (3H, Me), 3.88 s (3H, MeO), 3.92 s (6H, 2MeO), 5.10 s (2H, CH_2), 7.12 s (2H, arom), 7.31 d, 9.91 d (4H, J = 8.84 Hz, arom)
18	3.79 s (3H, Me), 3.82 s (6H, 2Me), 5.15 s (2H, CH_2), 7.08–8.09 m (11H, arom)
19	3.71 s (3H, Me), 3.82 s (6H, 2Me), 5.08 s (2H, CH_2), 7.11–8.43 m (6H, arom)
20	3.78 s (3H, Me), 3.83 s (6H, 2Me), 5.11 s (2H, CH_2), 7.11 s (2H, arom), 7.52 d, 8.09 d (4H, J = 8.85 Hz, arom)
21	3.82 s (3H, Me), 3.90–3.91 m (12H, 4Me), 5.0 s (2H, CH_2), 6.94–7.77 m (5H, arom)
22	3.72 s (3H, Me), 3.80 s (6H, 2Me), 5.29 s (2H, CH_2), 7.18–8.16 m (9H, arom)
23	3.8 s (3H, Me), 3.90 s (6H, 2Me), 5.20 s (2H, CH_2), 7.25–8.78 m (7H, arom)
24	7.50–8.10 m (11H, CHBr, arom)
25	3.58–4.29 m (6H, $3CH_2$), 6.90–8.11 m (8H, arom), 10.27 s (1H, OH)
26	3.72–4.29 m (6H, $3CH_2$), 6.88–8.03 m (11H, arom), 10.35 s (1H, OH)
27	3.74–4.18 m (6H, $3CH_2$), 6.96–7.80 m (8H, arom), 10.27 s (1H, OH)
28	3.70–4.15 m (6H, $3CH_2$), 7.00–7.88 m (10H, arom)
29	3.74–4.11 m (6H, $3CH_2$), 6.89–7.80 m (9H, arom), 10.26 s (1H, OH)
30	1.35 t (3H, Me, J = 7.1 Hz), 3.75–4.21 m (8H, $4CH_2$), 7.11 d, 7.90 d (4H, J = 8.84 Hz, arom), 7.26–7.55 m (5H, arom)
31	3.81 s, 3.82 s (6H, 2Me), 3.72–4.16 m (6H, $3CH_2$), 6.82–7.84 m (8H, arom)
32	3.35 s (3H, 2Me), 3.67–4.18 m (6H, $3CH_2$), 6.96–7.95 m (8H, arom)
33	3.73 s (3H, Me), 3.83 s (2H, CH_2S), 3.66–4.17 m (4H, dioxolane), 6.56–7.88 m (8H, arom), 10.30 s (1H, OH)
34	3.70 s, 3.75 s (6H, 2Me), 3.94 s (2H, CH_2S), 3.70–4.19 m (4H, dioxolane), 6.82–7.84 m (8H, arom), 10.34 s (1H, OH)
35	3.70 s (3H, Me), 3.89 s (6H, 2Me), 3.67–4.18 m (6H, $3CH_2$), 7.45–8.47 m (6H, arom)
36	3.65 s (3H, Me), 3.67 s (6H, 2Me), 3.54–4.16 m (6H, $3CH_2$), 7.40–8.21 m (6H, arom)
37	3.77 s (3H, Me), 3.82 s (6H, 2Me), 3.54–4.16 m (6H, $3CH_2$), 7.08–8.05 m (6H, arom)
38	3.82 s (3H, Me), 3.83–3.86 m (9H, 3Me), 3.54–4.16 m (6H, $3CH_2$), 7.26–8.0 m (6H, arom)
39	3.73 s (3H, Me), 3.84 s (5H, Me, CH_2S), 3.50–4.22 m (4H, dioxolane), 6.83–7.95 m (8H, arom)

reflect one or more atomic properties (represented by a separate value or by a vector of characteristics). Off-diagonal elements characterize bonds between pairs of atoms, if they exist, or distances otherwise. Usually, only the upper triangle of each matrix is used in calculations due to the symmetry of bonds. Also, more than one property can be taken for bonds. For the sake of simplification, the ETM calculations generally use only by one property for atoms and bonds. In cases where there are more than one property for atoms and bonds, the ETM calculations can be repeated separately for each property. In our case, effective charges on atoms are taken as diagonal elements, and the values of Wiberg's index represent off-diagonal elements corresponding to bonds; if no bond, then off-diagonal elements are distances for corresponding pairs of atoms.

The computational part of the ETM is a sequence of the following steps:

- Conformational analysis,
- Quantum-chemistry calculations,
- ETMC formation,
- The search for structural features, responsible for a compound's activity/inactivity (the features are referenced as pharmacophores/anti-pharmacophores, correspondingly). To find pharmacophores, a template *active* compound and the rest of the compound

set are compared as weighted graphs. To find anti-pharmacophores, an *inactive* compound is used as a template for the comparison. At the same time, the molecular flexibility is taken into account by the comparison of atomic and bond weights.

The last two steps represent the essential part of the ETM. The main advantages of the ETM are that its molecular descriptions reflect a molecule's electronic and 3D conformational properties and do not depend on the numbers and types of atoms.

Thus, for each template compound (active or inactive), its ETMC was compared with the ETMCs of the rest of the compounds in both classes of the series taken for this study. The comparison resulted in a few common structural fragments for the two cases. The fragments were found as submatrices of the ETMCs corresponding to templates (they will be referenced as electron-topological submatrices of contiguity, or ETSCs). Consequently, all pharmacophores and anti-pharmacophores found from the ETM calculations form a system for the activity identification. For the series studied, the system includes 15 pharmacophores and 10 anti-pharmacophores. From compound **11**, the chosen active template compound, an activity feature 1 (or the Ph1 pharmacophore) was found. It is given in Figure 1 with the corresponding ETSC, which describes electronic-topological characteristics of the fragment (see Fig. 1).

As seen from the Ph1 pharmacophore structure, it consists of 7 atoms (C_1, C_7, C_{16}–C_{19}), which relate structurally to the phenyl attached to the oxadiazole ring. The submatrix given in Figure 1 is found after setting allowable limits for finding equivalent matrix elements. The limits are $\delta_1 = \pm 0.05$ for its diagonal elements and $\delta_2 = \pm 0.15$ for the off-diagonal ones. The pharmacophore found from the ETM-calculations is realized in nine active compounds, and the probability P_A of its realization in this class is about 0.91.

One common criterion for structural methods (C_A) that evaluates the *probability* of occurrence of a pharmacophore (Ph) in the series under study is given by the following equation:

$$C_A(\mathrm{Ph}) = (n_A + 1)/(n_A + n_{IA} + 2), \quad (1)$$

where n_A, n_{IA} are numbers of active/inactive compounds, respectively, that contain the Ph. For an anti-pharmacophore (APh), (n_{IA}+1) is to be used at place of (n_A+1) in Eq. 1. The remaining pharmacophores, Ph2–Ph15, were found analogously, and the probabilities of their realization in the class of active compounds varied between 0.86 and 0.95.

To determine anti-pharmacophores, ETMCs of inactive compounds were taken as templates. Fifteen anti-pharmacophores, APh1–APh10, were found overall. The ETSCs that correspond to APh1 are given in Figure 2 along with structures of the corresponding template after which the anti-pharmacophore is found.

As seen from Figure 2, APh1 (based on the inactive template **33**) consists the nine atoms. APh1 is present in 10 inactive molecules and 1 active molecule, and the probability of its realization is 0.85.

When comparing the structures of the pharmacophores and anti-pharmacophores, one should pay close attention to the differences in their spatial and electronic characteristics. Thus, the pharmacophores and anti-pharmacophores when considered as a whole play an important role in activity predictions and the search for new drugs. The set of activity/inactivity fragments found as a result of this study forms a basis for the development of a system for anti-tuberculosis activity prediction.

4. Neural network application

Artificial neural networks (ANNs) comprise a group of methods that are increasingly being used in drug design to study quantitative/qualitative SAR (QSAR). This approach is able to elucidate SARs and account for any non-linear character of these relationships. Thus, this method can be of significant interest in three-dimensional (3D) QSAR studies.

C1	N7	C16	C17	C18	C19	C20
-0.04	2.57	1.36	1.37	2.42	2.80	2.42
	-0.08	3.79	3.08	4.47	5.26	4.98
		-0.09	2.43	2.80	2.42	1.44
			-0.08	1.43	2.42	2.79
				-0.14	1.41	2.41
					-0.10	1.40
						-0.14

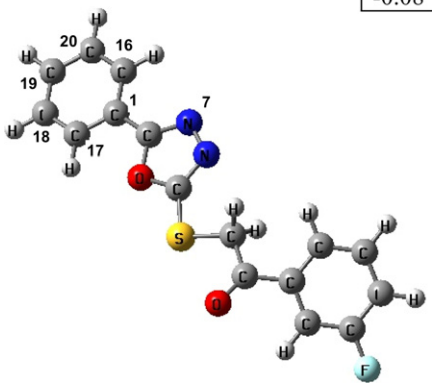

Figure 1. The Ph1 pharmacophore found relative to active molecule **11.**

O3	N7	C8	C9	O11	O12	C19	C20	O27
-0.12	2.25	4.02	4.72	4.27	5.90	5.46	6.43	6.38
	-0.08	4.45	5.01	4.28	5.77	5.00	5.98	6.60
		-0.32	0.93	2.45	2.37	3.55	3.53	10.36
			0.25	0.95	0.94	2.35	2.35	10.85
				-0.28	2.28	0.96	2.35	9.97
					-0.29	2.34	0.97	11.95
						-0.04	0.96	10.77
							-0.05	12.08
								-0.25

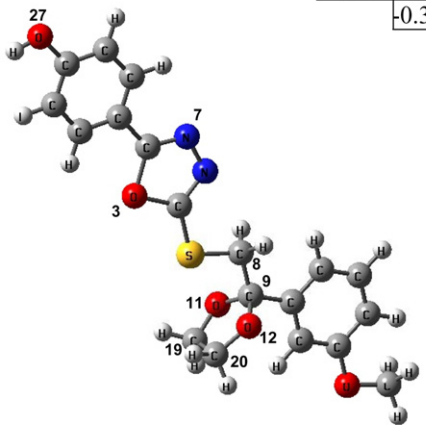

Figure 2. The AP1 anti-pharmacophore found relative to inactive molecule **33**.

The architecture of the artificial supervised NN applied to our study consists of three-layers, with five neurons in one hidden layer. A single output node was used to code activities of inhibitors. The bias neurons were presented on the input and hidden layers. At least $M = 200$ independent FFNNs were trained to analyze each set of variables. The values predicted for each analyzed case were averaged over all M network predictions, and the means were used to calculate statistical coefficients for targets. Further details of the algorithm can be found elsewhere.[28,29]

The avoidance of overfitting/overtraining has been shown to be an important factor for improving the predictive ability and correct selection of variables in the FFNNs. The early stopping over ensemble (ESE) technique was used in the current study to achieve this end. We used a subdivision of the initial training set into two equal learning/validation subsets. The first set was used to train the neural network, while the second was used to monitor the training process measured by root mean square error. An *early stopping point* determined as a best fit of the network to the validation set was used to stop the neural network learning. Thus, statistical parameters calculated at the early stopping point were used. The training was terminated by limiting the network run to 10,000 epochs (*total* number of epochs) or after 2000 epochs (*local* number of epochs) following the last improvement of root-mean-square error in the early stopping point. The root-mean-square error E was computed as a criterion for network learning to determine the stop points of the training procedure. The quality of the model was tested by the leave-one-out (LOO) cross-validation procedure carried out on the training set with q^2 value (Cramer et al.[30]) and is defined as

$$q^2 = (SD - press)/SD. \quad (2)$$

In Eq. 2, SD represents the variance of a target value relative to its mean and '*press*' is the average squared errors of predicted values obtained from the LOO procedure.

The LOO cross-validation procedure that supervises the predictive performance of the ANN, has shown that pruning algorithms[31,32] can be used to optimize the number of input parameters for the ANNs training and to select the most significant ones. These algorithms operate in a manner similar to step-wise multiple regression analysis and, at each step, exclude by one input parameter that has been estimated as non-significant.[31–34] The pruning algorithms were used in the current study to determine significant parameters from the input data points of the analyzed molecules, as described in the references.

As the second stage, we examined whether all 25 molecular fragments (pharmacophores and anti-pharmacophores) are relevant for the anti-tuberculosis activity prediction. For these 25 fragments and 41 compounds in the series studied, a table of weights was formed as consisting of 41 rows of 25 elements being 1 (the fragment is present in the corresponding molecular structure) or 0 (the fragment is absent).

Application of pruning methods allowed for the selection of only five of the most appropriate parameters responsible for the anti-tuberculosis inhibitory activity.

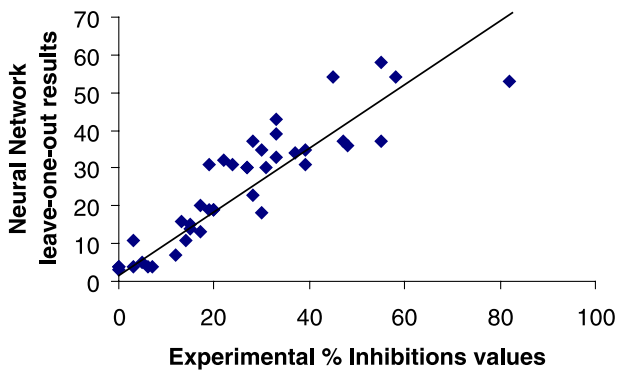

Figure 3. Theoretical and experimental % inhibitions results.

The reduction of the initially selected seven parameters to five did not decrease the cross-validated q^2 coefficient (0.80 ± 0.01). As illustrated in Figure 3, there was a good concordance between the predicted and experimental values of the anti-tuberculosis activities.

This result confirms our hypothesis in that both pharmacophores and anti-pharmacophores must be considered as parameters when building a model for anti-tuberculosis activity prediction.

5. Conclusions

A series of 2,5-disubstituted-1,3,4-thiadiazoles were designed and synthesized, and these compounds were screened for anti-tuberculosis activity against *M. tuberculosis* $H_{37}Rv$. A systematic SAR study was performed through application of the ETM approach to the series of compounds relative to their experimentally measured anti-tuberculosis activity. Data obtained from conformation and quantum-chemistry calculations were used to form electronic-topological matrices. These matrices were effectively used in the search for a system of pharmacophores and anti-pharmacophores capable of effective separation of compounds from the examination set into groups of active and inactive compounds. Low activity molecules are badly responsive to the activity prognostication, because they form a buffer zone consisting of compounds that can include both pharmacophores and anti-pharmacophores. The model developed in this study is supposed to be applied to the design, preparation and screening of new compounds of similar structure in order to further test and optimize the model with the eventual goal of preparing new anti-tubercular agents.

6. Experimental

6.1. Chemical methods

All the solvents used were reagent quality, and all commercial reagents were used without additional purification. Removal of all solvents was carried out under reduced pressure. Physical and analytical data of the synthesized compounds **3a**–**41** are given in Table 2. Analytical TLC plates were Silufol® UV-254 (Silpearl on aluminium foil, Czecho-Slovakia). IR spectra were recorded on a Specord 75 IR instrument (suspension in Vaseline oil). Melting points (uncorrected) were determined on a Boetius apparatus. ^{1}H NMR spectra were recorded for d_6-DMSO solution on a Varian XL-400 spectrometer (399.95 MHz) and a Bruker AC-80 (80 MHz) apparatus and are given in Table 3. Mass spectra were recorded on a Finnigan MAT.INCOS-50 instrument (ionizing voltage 70 eV).

6.1.1. Precursors of compounds 7–23, 25–39. The starting ω-phenacyl bromides and 2-bromomethyl-2-phenyl-1,3-dioxolanes were obtained according to the published methods.[35–39] The arylhydrazines **3a**–**j** have been prepared from esters **2a**–**j** and were used to prepare the 1,3,4-oxadiazoles **4a**–**j** according to a known procedure.[26]

6.1.2. General procedure for the preparation of the thioethers 5–23. Et_3N (0.303 g, 3 mmol) was added to a suspension of (3 mmol) 1,3,4-oxadiazole in 15 mL of acetone. To the resulting homogeneous solution, the appropriate ω-phenacyl bromide or MeI (3 mmol) was added as one portion. The reaction mixture was stirred for 1 h at 40 °C. When the reaction was completed (TLC control), the precipitate was filtered and crystallized from the appropriate solvent.

6.1.3. Synthesis of 2-bromo-1-phenyl-2-(5-phenyl-1,3,4-oxadiazol-2-ylsulfanyl)-1-ethanone 24. To a solution of **7** (2.96 g, 0.01 mol) in CCl_4 (30 mL) and NBS (1.96 g, 0.011 mol) 200 mg of benzoyl peroxide were added. The mixture was refluxed for 2 h (TLC control). The reaction mixture was purified over a short plug of silica (5 g). After evaporation of the solvent under reduced pressure, the crude product **24** (yield 3.37 g, 90%) was used without purification in the next step. IR (ν/cm^{-1}): the sample (**24**) in liquid paraffin showed absorption in the region 650 (Br—C) and 1780 (C=O).

6.1.4. General procedure for the preparation of the thioethers 25–39. 5-Aryl-1,3,4-oxadiazole (3 mmol) in 5 mL DMF and 0.62 g (4.5 mmol) of potassium carbonate were placed into a 3-necked round bottom flask, equipped with thermometer, stirrer, and condenser. The mixture was stirred for 5 min, and of 2-bromomethyl-2-phenyl-1,3-dioxolane (3 mmol) was added. The reaction temperature was increased to 130 °C , and the mixture was stirred for 3 h (TLC control). The cooled reaction mixture was poured into 50 mL of water while stirring. The resulting precipitate was filtered, washed with water, dried, and crystallized from the specified solvent (Table 2).

6.1.5. Synthesis of 3-(4-bromophenyl)-1-phenyl-2-(5-phenyl-1,3,4-oxadiazol-2-ylsulfanyl)-2-propen-1-one 40. To a solution of **7** (2.96 g, 0.01 mol) in toluene (50 mL) and 4-bromobenzaldehyde (1.85 g, 0.01 mol), 50 mg of pyrrolidine and 50 mg acetic acid were added. The mixture was refluxed with Dean-Stark apparatus for 15 h. The reaction mixture was washed with water (3×50 mL) and dried ($MgSO_4$). After removal of the toluene, the solid was crystallized from EtOH. IR (ν/cm^{-1}): 650 (Br—C) and 1675 (C=O). ^{1}H NMR (δ, ppm): 7.35 s (1H, CH=), 7.40–8.0 m (14H, arom). MS, *m*/*z* (relative intensity %): 462 $[M]^+$(25), 359(5), 285(35), 212(15), 178(35), 145(50), 105(90), 89(15), 77(100).

6.1.6. Synthesis of 4-phenyl-5-(5-phenyl-1,3,4-oxadiazol-2-ylsulfanyl)-1,3-thiazol-2-amine 41. To a solution of **24** (1.87 g, 0.005 mol) in EtOH (20 mL), thiourea (0.76 g, 0.005 mol) in 10 mL of EtOH was added. The mixture was refluxed for 1 h. After evaporation of EtOH under reduced pressure, the residue was suspended in a 10% solution of $NaHCO_3$ and heated to 50 °C. The crystalline product was filtered, washed with water, and crystallized from EtOH to give the final 2-aminothiazole **41** (1.54 g, 88%) as a white powder. IR (ν/cm^{-1}):

3450 (NH_2). ^1H NMR (δ, ppm): 5.97 w s (1H, CH=), 7.14–8.21 m (10H, arom). MS, *m/z* (relative intensity %): 352 $[M]^+$(100), 207(30), 165(70), 145(70), 133(5), 121(20), 103(20), 89(20), 77(50), 60(5).

6.1.7. In vitro evaluation of the anti-mycobacterial activity. Primary screening was conducted at 6.25 μg/mL against *M. tuberculosis* $H_{37}Rv$ (ATCC 27294) in BACTEC 12B medium using a broth microdilution assay, the Microplate Alamar Blue Assay (MABA) according to the reported method.[15]

Acknowledgments

The authors gratefully acknowledge funding through a grant from the Moldavian–U.S. Bilateral Grants Program of the U.S. Civilian Research and Development Foundation (Grant MC2-3007). The authors also acknowledge the Tuberculosis Antimicrobial Acquisition and Coordinating Facility provided through the U.S. National Institutes of Health (Contract N01-AI-95364) for providing the anti-tubercular activity data.

References and notes

1. World Health Organization. In *Anti-tuberculosis Drug Resistance in the World*; The WHO/IUATLD global project on anti-tuberculosis drug resistance surveillance, 1997.
2. Bastian, I.; Colebunders, R. *Drugs* **1999**, *58*, 633–661.
3. Butler, D. *Nature* **2000**, *406*, 670–672.
4. Bodiang, C. K. *Scott. Med. J.* **2000**, *45*, 25.
5. Van Scoy, R. E.; Wilkowske, C. *J. Mayo Clin. Proc.* **1999**, *74*, 1038.
6. Long, R. *Can. Med. Assoc. J.* **2000**, *163*, 425–428.
7. Gazdic, A. *Med. Arch.* **1998**, *52*, 207.
8. Pozniak, A. *Int. J. Tuberc. Lung Dis.* **2000**, *4*, 993.
9. Poroikov, V. V.; Filimonov, D. A.; Borodina, Yu. V.; Lagunin, A. A.; Kos, A. *J. Chem. Inf. Comput. Sci.* **2000**, *40*, 1349–1355.
10. Stepanchikova, A. V.; Lagunin, A. A.; Filimonov, D. A.; Poroikov, V. V. *Curr. Med. Chem.* **2003**, *10*, 225.
11. Poroikov, V. V.; Filimonov, D. A. *J. Comput. Aided Mol. Des.* **2003**, *16*, 819–824.
12. Geronikaki, A. A.; Dearden, J. C.; Filimonov, D.; Galaeva, I.; Garibova, T. L.; Gloriozova, T.; Krajneva, V.; Lagunin, A.; Macaev, F. Z.; Molodavkin, G.; Poroikov, V. V.; Pogrebnoi, S. I.; Shepeli, F.; Voronina, T. A.; Tsitlakidou, M.; Vlad, L. *J. Med. Chem.* **2004**, *47*, 2870–2876.
13. Geronikaki, A.; Babaev, E.; Dearden, J.; Dehaen, W.; Filimonov, D.; Galaeva, I.; Krajneva, V.; Lagunin, A.; Macaev, F.; Molodavkin, G.; Poroikov, V.; Pogrebnoi, S.; Saloutin, V.; Stepanchikova, A.; Stingaci, E.; Tkach, N.; Vlad, L.; Voronina, T. *Bioorg. Med. Chem.* **2004**, *12*, 6559–6568.
14. Oruç, E.; Rollas, S.; Kandemirli, F.; Shvets, N.; Dimoglo, A. S. *J. Med. Chem.* **2004**, *47*, 6760–6767.
15. Collins, L.; Franzblau, S. G. *Antimicrob. Agents Chemother.* **1997**, *41*, 1004–1009.
16. Dimoglo, A. S.; Sim, E.; Shvets, N. M.; Ahsen, V. *Mini Rev. Med. Chem.* **2003**, *3*, 293.
17. Dimoglo, A. S.; Shvets, N. M.; Tetko, I. V.; Livingstone, D. J. *Quant. Struct.-Act. Relat.* **2001**, *20*, 31.
18. Dimoglo, A. S. *Khim.- pharm. Zhur.* **1985**, *4*, 438.
19. Bersuker, I. B.; Dimoglo, A. S. The electron-topological approach to the QSAR problem. In *Reviews in Computational Chemistry*; Lipkowitz, K. B., Boyd, D. B., Eds.; VCH: New York, 1991, Chapter 10.
20. Shvets, N. M.; Dimoglo, A. S. *Nahrung* **1998**, *42*, 364.
21. Dimoglo, A. S.; Beda, A. A.; Shvets, N. M.; Gorbachov, M. Yu.; Kheifits, L. A.; Aulchenko, I. S. *N. J. Chem.* **1995**, *19*, 149.
22. Dimoglo, A. S.; Vlad, P. F.; Shvets, N. M.; Coltsa, M. N. *N. J. Chem.* **2001**, *25*, 283.
23. Shvets, N. M.; Dimoglo, A. S. The electronic-topological method (ETM): its further development and use in the problems of SAR study. In *Molecular Modeling and Prediction of Bioactivity*; Gundertofte, K., Jorgensen, F. S., Eds.; Kluwer Academic/Plenum Publishers: New York, 1999, p 418.
24. Kohonen, T. *Self-organisation Maps*; Springer-Verlag: Berlin, 1995.
25. Simon, V.; Gasteiger, J.; Zupan, J. A. *J. Am. Chem. Soc.* **1993**, *115*, 9148–9159.
26. Rusu, G. G.; Gutu, E. E.; Barba, N. A. *Russ. J. Org. Chem.* **1995**, *31*, 1721.
27. Frisch, M. J.; Trucks, G. W.; Schlegel, H. B. et al. Gaussian 98, Revision A.9, Gaussian, Inc., Pittsburgh, PA, 1998.
28. Kovalishyn, V. V.; Tetko, I. V.; Luik, A. I.; Kholodovych, V. V.; Villa, A. E. P.; Livingstone, D. J. *J. Chem. Inf. Comput. Sci.* **1998**, *38*, 651–659.
29. Tetko, I. V.; Livingstone, D. J.; Luik, A. I. *J. Chem. Inf. Comput. Sci.* **1995**, *35*, 826–833.
30. This coefficient was introduced as r^2 in Cramer III, R. D.; Patterson, D. E.; Bunce, J. D. *J. Am. Chem. Soc.* **1988**, *110*, 5959–5967. However, in order to avoid confusion with the analogous conventional $r^2 = R * R$ value the new designation q^2 was recommended in Cramer III, R. D.; De Priest, S. A.; Patterson, D. E.; Hecht, P. The Developing Practice of Comparative Field Analysis. In *3D QSAR in Drug Design: Theory Methods and Applications*; Kubinyi, H., Ed.; ESCOM: The Netherlands, 1993, pp 443–486.
31. Tetko, I. V.; Villa, A. E. P.; Livingstone, D. J. *J. Chem. Inf. Comput. Sci.* **1996**, *36*, 794–803.
32. Tetko, I. V. *J. Chem. Inf. Comput. Sci.* **2002**, *42*, 717–728.
33. Tetko, I. V.; Kovalishyn, V. V.; Livingstone, D. J. *J. Med. Chem.* **2001**, *44*, 2411–2420.
34. Tetko, I. V.; Kovalishin, V. V. http://146.107.217.178/lab/asnn/index.html.
35. Ma, Y.; Liu, H.; Chen, L.; Cui, X.; Zhu, J.; Deng, J. *Org. Lett.* **2003**, *5*, 2103.
36. Kim, Y. H.; Cheong, C. S.; Lee, S. H.; Jun, S. J.; Kim, K. S.; Cho, H. S. *Tetrahedron Asymmetry* **2002**, *13*, 2501–2508.
37. Adhikari, M. V.; Samant, S. D. *Ultrason. Sonochem.* **2002**, *9*, 107.
38. Camps, P.; Farres, X. *Tetrahedron Asymmetry* **1995**, *6*, 1283–1294.
39. Sket, B.; Zupan, M. *Synth. Commun.* **1989**, *19*, 2481–2487.